



**HAL**  
open science

## Behaviour of the CO<sub>2</sub> injection well and the near wellbore during carbon dioxide injection in saline aquifers

Mohamed Azaroual, Laurent André, Yannick Peysson, Jacques Pironon, Daniel Broseta, Fabian Dedecker, Patrick Egermann, Jean Desroches, Joëlle Hy-Billiot

► **To cite this version:**

Mohamed Azaroual, Laurent André, Yannick Peysson, Jacques Pironon, Daniel Broseta, et al.. Behaviour of the CO<sub>2</sub> injection well and the near wellbore during carbon dioxide injection in saline aquifers. TOUGH Symposium 2012, Sep 2012, Berkeley, United States. pp.Session V: Carbon Dioxide Storage II. hal-00755073

**HAL Id: hal-00755073**

**<https://brgm.hal.science/hal-00755073v1>**

Submitted on 20 Nov 2012

**HAL** is a multi-disciplinary open access archive for the deposit and dissemination of scientific research documents, whether they are published or not. The documents may come from teaching and research institutions in France or abroad, or from public or private research centers.

L'archive ouverte pluridisciplinaire **HAL**, est destinée au dépôt et à la diffusion de documents scientifiques de niveau recherche, publiés ou non, émanant des établissements d'enseignement et de recherche français ou étrangers, des laboratoires publics ou privés.

## BEHAVIOUR OF THE CO<sub>2</sub> INJECTION WELL AND THE NEAR WELLBORE DURING CARBON DIOXIDE INJECTION IN SALINE AQUIFERS

Mohamed AZAROUAL<sup>1</sup>, Laurent ANDRE<sup>1</sup>, Yannick PEYSSON<sup>2</sup>, Jacques PIRONON<sup>3</sup>, Daniel BROSETA<sup>4</sup>, Fabian DEDECKER<sup>5</sup>, Patrick EGERMANN<sup>6</sup>, Jean DESROCHES<sup>7</sup>, Joëlle HY-BILLIOT<sup>8</sup>

<sup>1</sup> BRGM, Water Division, 3 Avenue Claude Guillemin, BP 36009, F-45060 ORLEANS Cedex 2 France

<sup>2</sup> IFP Energies nouvelles, 1-4 avenue de Bois Préau, 92852 Rueil-Malmaison Cedex - France

<sup>3</sup> Université de Lorraine, CNRS, G2R laboratory, BP 70239, 54506 Vandœuvre-lès-Nancy, France

<sup>4</sup> UMR 5150, LFCR, Université de Pau & Pays Adour, BP 1155, 64013 PAU Cedex, France

<sup>5</sup> ITASCA Consultants, S.A.S., 64 Chemin des Mouilles, 69130 ECULLY, France

<sup>6</sup> GDF SUEZ, STORENGY, 12 rue Raoul Nordling, 92270 Bois Colombes, France

<sup>7</sup> SCHLUMBERGER, Etudes et Productions Schlumberger, SRPC, 1 rue Henri Becquerel, 92142 Clamart, France

<sup>8</sup> TOTAL E&P, DGEP/SCR/RD/MGR, Avenue Larribau, 64018 PAU CEDEX, France

e-mail: [m.azaroual@brgm.fr](mailto:m.azaroual@brgm.fr); [l.andre@brgm.fr](mailto:l.andre@brgm.fr); [yannick.peysson@ifpen.fr](mailto:yannick.peysson@ifpen.fr); [jacques.pironon@univ-lorraine.fr](mailto:jacques.pironon@univ-lorraine.fr); [daniel.broseta@univ-pau.fr](mailto:daniel.broseta@univ-pau.fr); [f.dedecker@itasca.fr](mailto:f.dedecker@itasca.fr); [patrick.egermann@storengy.com](mailto:patrick.egermann@storengy.com); [JDesroches1@slb.com](mailto:JDesroches1@slb.com); [Joelle.HY-BILLIOT@total.com](mailto:Joelle.HY-BILLIOT@total.com).

### **ABSTRACT**

The project "*Proche Puits*" ("Near Wellbore") co-funded by the French National Agency for Research (ANR) started in December 2007 and ended in May 2011. The project consortium gathered three companies (TOTAL, Schlumberger, and GDF-Suez), two applied research institutes (BRGM and IFP Energies nouvelles), two academic research laboratories (CNRS and Université de Lorraine) and a SME (ITASCA). The main processes studied were: i) physical behaviour of flowing fluids (CO<sub>2</sub>) in the well and their impacts on the bottom hole T-P conditions, ii) thermo-kinetic effects on the petrophysical and physico-chemical processes, iii) drying-out of the near-wellbore porous media and reactivity of highly evaporated residual brines retained by capillary and osmotic forces in the pores, and iv) petrophysical and geomechanical impacts of coupled processes.

The understanding of these phenomena based on laboratory experiments and numerical modelling allowed a better interpretation of the coupled processes and the development of advanced concepts of CO<sub>2</sub> storage in saline aquifers. The project demonstrates firstly that injection of large quantity of CO<sub>2</sub> in deep saline aquifers will lead to a strong water desaturation of the near wellbore because of drying mechanisms. In this context, drying mechanisms can precipitate the salt present in the aquifer and then lead to

injectivity alteration due to permeability decrease.

Numerical modelling coupling hydraulic and thermal processes were shown to be able to simulate the observed evolution of liquid and gas saturations and to estimate the salt depositions. The numerical simulations approaches were validated with respect to laboratory experiments in controlled conditions allowing the determination of the most important parameters for injectivity design (porosity, relative permeability and capillary pressure curves...). The experimental observations, established at the centimetre scale, were up-scaled in order to extrapolate the results at the near wellbore scale and then, to forecast the impact of CO<sub>2</sub> injection on petrophysical properties of the host rock.

Finally, obtained results allow the definition of recommendations and risk analyses on the injectivity for CO<sub>2</sub> geological storage in aquifer. Injection flow rates, optimum pressure and temperature in wells can then be evaluated to avoid damage in the near wellbore zone and maintain injectivity during the life-period of the well exploitation.

### **INTRODUCTION**

The "*Near Wellbore*" project was focused on the study of main physical, physicochemical and thermo-kinetic phenomena occurring in the well and the near wellbore domain. The understanding of these phenomena based on

scientific and technical knowledge will reduce the uncertainties on the injectivity and the predictive results of numerical simulations on the sustainability and security of CO<sub>2</sub> storage. This knowledge will also help to identify ranges of CO<sub>2</sub> storage capacity in saline aquifers.

Indeed, it is now established that the amount and the quality of the injected CO<sub>2</sub> play a key role on the preservation of the injectivity of the reservoir and on the number and type of required injection wells. On the other hand, depth, location, temperature and pressure conditions, and petrophysical characteristics of the targeted reservoir, as well as the quality of the caprock are parameters that must be characterized because of their influence on the required number of wells, on the evolution of the injectivity and on the technical management of the conditions of pressure at the wellhead and at the bottom of the well. Also, the multiphase area developing around the near well is a very sensitive and reactive zone where numerous coupled processes have been identified, including hysteretic behaviors, and may play a key role during the CO<sub>2</sub> injection phase as technical stop and restart stages will happen.

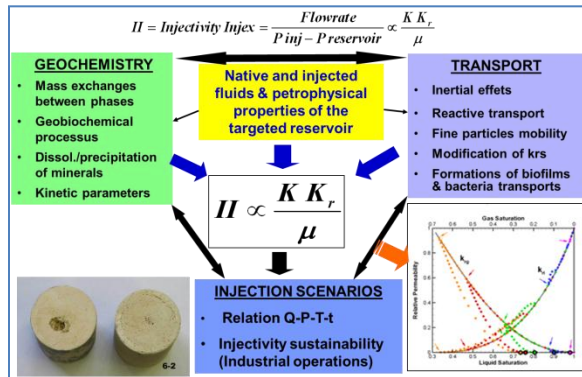


Figure 1. Coupled key processes to integrate in numerical tools to study the injection scenarios based on the control of relative permeabilities and interfacial mechanisms of mass and heat transfers between phases.

In summary, the integration of the empirical macroscopic parameter defined as the *Injectivity index*, *II*, (Figure 1) is the key condition of success of a CGS (Carbon Geological Storage) operation. This parameter expresses the behavior of the reservoir under imposed P-T-Q-t conditions, i.e. injection pressure (P), temperature (T), flow (Q) and their time

evolution (t). As illustrated in Figure 1, *II* primarily depends on the evolution of the relationship between water saturation (*S<sub>w</sub>*) of the porosity and relative permeability (*K<sub>r</sub>*). This relationship depends, in turn, on the properties of the injected fluids and on the characteristics of the target reservoir rock (bio- and geochemical reactivity, initial petrographic and hydrodynamic properties ...).

### MULTIPHASE REACTIVE TRANSPORT AND NEAR WELLBORE BEHAVIOR

Based on recent numerical and experimental simulations, the near-well injection zone is identified to be particularly impacted by supercritical CO<sub>2</sub> injection and the most sensitive area (André et al., 2007; 2010), where chemical (e.g., mineral dissolution/precipitation) and physical (e.g., temperature, pressure and gas saturation) phenomena have a major impact on the porosity and permeability and thus, at the end, on the well injectivity.

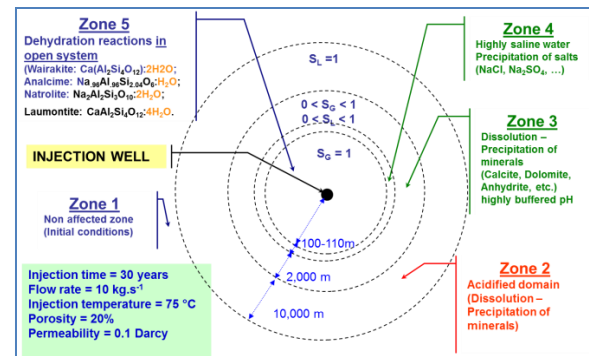


Figure 2. Typical fictive radii of the processes occurring in the near well region after a continuous injection of CO<sub>2</sub> during 30 years with a flow rate of 1 Mm<sup>3</sup>/y (André et al., 2007; Gaus et al. 2008).

Figure 2 represents the simulation result of two-phase reactive transport (CO<sub>2</sub> - initially porous carbonate rock saturated with water) using TOUGHREACT (Xu et al., 2004) showing the individualization and the succession of five (5) major zones of specific physical and physico-chemical properties around the injection well. These zones have the following characteristics:

- Zone 1 (initial unperturbed state): the porous medium contains only the initial aqueous solution. The pores are saturated with water (initial state) under conditions of thermodynamic

equilibrium between minerals of the rock matrix and pore water.

- Zone 2 (monophasic acidified zone): pH decreases due to CO<sub>2</sub> dissolution (forming carbonic acid H<sub>2</sub>CO<sub>3</sub>) in the aqueous phase. The porous medium is still saturated with water. This is a more acidic front before the arrival of supercritical CO<sub>2</sub> phase. This solution at lower pH is aggressive for most of the porous matrix minerals, including carbonates and to a lesser degree aluminosilicates.

- Zone 3 (multiphase zone): the porosity of the porous medium contains two phases, namely the aqueous phase and the supercritical CO<sub>2</sub>. The pH and the composition of the aqueous phase vary with water saturation with a drying trend of the rock and creating conditions for capillarity.

- Zone 4 (dried zone): pH and ionic strength increase sharply due to the drying-out of the medium. This produces a strong tendency of the system triggering reactive mass exchange processes between major phases (residual water - supercritical CO<sub>2</sub> - minerals). The pore solutions become highly saline, with values of the ionic strength of about 7 to 7.5 (equivalent mol / kg H<sub>2</sub>O) although the initial aqueous solution was only at 0.1 (Zone 1).

- Zone 5 (extreme conditions of capillarity and dehydration reactions): the aqueous phase is totally removed and the porous medium contains only supercritical CO<sub>2</sub> and a small quantity of metastable and capillary water in the fine pores and microcracks.

The various physical phenomena and physicochemical predominantly of each zone were analyzed separately in the framework of the “*Near Wellbore*” project by implementing new measurement techniques and some new theoretical approaches. The integration of results from different disciplines allows understanding multiphase reactive transport inducing heat and mass transfers between phases.

### **The CO<sub>2</sub> injection well behavior: a “Pseudo” steady-state calculation example**

This test case was jointly run by Total and Schlumberger. It consists of a single-cased off-shore well, located in a shallow water zone (300m depth). The well is vertical, and its total depth is 1000m. The boundary conditions

(pressure, temperature and volumetric flow rate) are set at the wellhead. The injection temperature is set at 5°C, while the injection pressure is set at 100 bars. Several volumetric flow rates are considered: 500 t/day, 1000 t/day, 2000 t/day and 2750 t/day. The far field temperature in the formation varies linearly from 5°C at wellhead (0 m) to 21°C at 1000m. The geological formation was made of limestone and sandstone, but as the thermal parameters input were not available, we chose the same parameters for both layers, assuming it would not change much the results.

This example was tested by Schlumberger with PipeSIM, and by Total, with PROSPER, each software based on different theoretical approaches and practice assumptions. PipeSIM is only able to perform steady-state calculations, in contrast to PROSPER, which allows obtaining results for 10 days, 100 days and 1000 days after the start of injection. Considered times are, however, fairly large, and probably sufficiently close to steady-state to allow a meaningful comparison between the results of the two simulators. The codes provided fairly different results. Note that the pressure vs. temperature curve along the well calculated with PipeSIM looks suspicious (Figure 3): a brutal change of the slope occurs when the pressure exceeds a value ranging between 72 bars and 76 bars for the cases investigated (depending on the volumetric flow rate and the equation of state (EOS) considered for CO<sub>2</sub>).

The simulations carried out with PROSPER use the Peng-Robinson EOS (Peng-Robinson, 1976) to model the behavior of CO<sub>2</sub>. The simulator described here (NEW SIMULATOR) uses the Span-Wagner EOS (Span-Wagner, 1996). PipeSIM calculations are run using alternatively these two equations of state.

In the previous simulations, the convective heat transfer coefficient between tubing and the fluid inside it was considered constant (11 W.m<sup>-2</sup>.K<sup>-1</sup>) all along the well. This is not the case in reality, as the heat transfer coefficient is usually dependent on numerous parameters evolving with depth and time (e.g. the fluid velocity, density, viscosity). The heat exchange between the fluid and the pipe is often expressed by mean of a correlation, relating the Reynolds, Prandtl and Nusselt numbers of the flow. In the current

version of this new simulator, the correlation implemented is that of Gnielinski (62) - see Incropera (2001).

The temperature vs. pressure curves associated to each case are presented in Figure 3. The numbers in the caption are the flow rate values (in ton/day), while the two-letters acronyms 'SW' and 'PR' denote respectively 'Span-Wagner' and 'Peng-Robinson' (the equations of state of CO<sub>2</sub> used for the current case).

The present simulator is denoted 'NEWSIM' in the caption ('PipeSIM' and 'PROSPER' are self-explanatory). Figure 3 shows that the results obtained with the new simulator are much closer to those obtained with PROSPER than those obtained with PipeSIM. The associated curves do not exhibit the strange change in slope mentioned earlier, which tends to demonstrate a lack of coherence in the PipeSIM results. The new simulator predicts a temperature 10 to 13% lower than PROSPER, and a pressure slightly 4 to 5% higher.

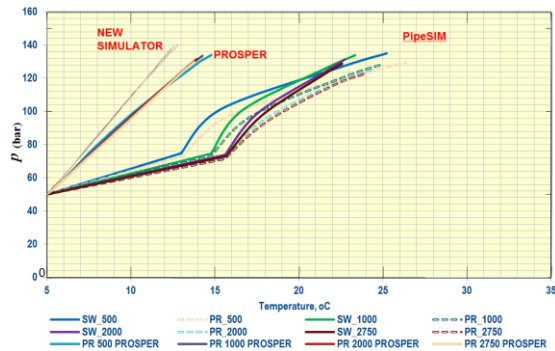


Figure 3. Pressure vs. Temperature curves obtained with the three simulators, considering four flow rates and two different equations of states.

To summarize, these discrepancies can be explained by one or a combination of the following reasons:

- The use of the Span-Wagner (1996) EOS instead of the Peng-Robinson (1976) EOS. This trend is similar to that observed in the PipeSIM results when one switches from one EOS to the other: the bottom-hole temperature sustains a 4% to 5% relative decrease, while the bottom-hole pressure increases 4 to 5%.
- The use of a variable CO<sub>2</sub>/tubing heat transfer coefficient (described by the

Gnielinski's correlation; see Incropera (2001)) instead of a constant one.

### The near wellbore dynamics

As shown in Figure 2, the desiccation of the porous medium appears as a major phenomenon with various consequences as salts precipitation (Peysson et al., 2010), modification of the local geomechanical constraints due to the salts precipitation, modification of internal forces and the impact of injected fluids on the interfacial tensions including capillary/osmotic phenomena. Desiccation of porous media submitted to gas injections is a well-known process at the laboratory (Mahadevan, 2005; Mahadevan et al., 2007) and the field (Kleinitz et al., 2003) scales. This process is taken into account only recently in the modelling of CO<sub>2</sub> storage in deep saline aquifers (André et al., 2007; Zeidouni et al., 2009).

First, the massive and continuous injection of CO<sub>2</sub> in a saturated porous medium involves water displacement and evaporation: mobile water is removed by the injected dehydrated supercritical CO<sub>2</sub> allowing tow phase flow system (brine – CO<sub>2</sub>). At the end, immobile residual water entrapped in pores or distributed on grain surface as a thin film, is in contact with the flowing dry CO<sub>2</sub> (i.e. with very low water vapor pressure). Consequently, a continuous and extensive evaporation process leads both to the apparition of a drying front moving into the medium, and the precipitation of salts and possibly secondary minerals in residual brines.

This study investigates the consequences on permeability degradation of the porous medium potentially induced by desiccation through the petrophysical properties of different subsystems. Experimental evaluations of drying of brine are investigated at the laboratory scale on centimetre plugs of different materials. These experiments are then interpreted using a numerical modelling approach coupling hydraulic and thermal processes able to simulate the evolution of liquid and gas saturations in space and in time. A very fine discretization of the plugs allows capturing the continuous evolution of water and gas profiles in the porous medium and estimating the liquid saturation and the permeability evolution during drying process.

The experiments of gas injection were performed on two materials:

- with a low permeability sandstone ("Grès de Môlière"  $\Phi=14.0\%$  and  $K_0=8\ \mu\text{D}$ ) in order to increase the capillary effects to be able to study them and quantify their effect. Indeed, those effects play a key role in drying processes,
- with a high permeability sandstone ("Grès des Vosges"  $\Phi=21.8\%$  and  $K_0=60\ \text{mD}$ ) in order to study rocks with properties close to the ones found in targeted reservoirs of  $\text{CO}_2$  storage.

Sandstones samples of 6 cm long initially saturated with brine (salinity of  $160\ \text{g L}^{-1}$ ) are placed in storage conditions ( $80^\circ\text{C}$ - $120^\circ\text{C}$  – 50 bars) and in a cell transparent to X-ray. Dry gas (nitrogen) is injected in the fully saturated core plugs (Figure 4). Four long pressure stages are imposed to desaturate progressively the rock plug. The local water saturation in the sample is measured with X-ray attenuation techniques. Pressure difference and outlet gas flow rate are monitored during the experiment. The system evolves until complete drying. The experiments were performed at 90 and  $120^\circ\text{C}$  with "Grès de Môlière" samples and at  $90^\circ\text{C}$  for "Grès des Vosges" core.

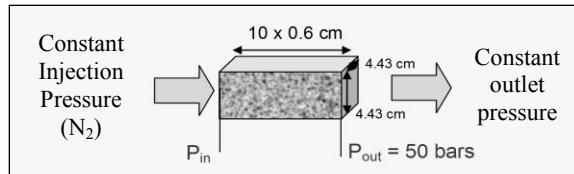


Figure 4. Experimental procedure to investigate the drying out of the core under a continuous flux of nitrogen.

### **Numerical simulation of multiphase flow and drying-out (lab scale)**

The TOUGH2 simulator (Pruess et al., 1999) with the EOS7C module (Oldenburg et al., 2004) was used for all the simulations carried out for this study (core experiments and field scale). This code couples thermal and hydraulic processes and is applicable to one-, two-, or three-dimensional geologic systems with physical heterogeneity. The EOS7C is a fluid property module developed specifically to deal with mixtures of non-condensable gases (like  $\text{CO}_2$  or  $\text{N}_2$ ) and methane. It can be used to model isothermal or non-isothermal multiphase flow in water/brine/ $\text{CH}_4$ /( $\text{CO}_2$  or  $\text{N}_2$ ) systems.

Modelling approach consists to simulate the injection of nitrogen in a plug fully saturated with water. A two-phase Darcy flow is solved using relative permeability and capillary pressure curves. Thermodynamic equilibrium between concomitant phases (brine –  $\text{N}_2$ ) is calculated at each time step to evaluate the water vapour fraction in the gas and the dissolved gas in the brine.

A 1D column model of 6 cm long is used as a conceptual framework for determining the evolution of the water content induced by the injection of  $\text{N}_2$ , in both time and space. The column is represented by 10 grid blocks composing the model mesh. The thickness of each grid cell is constant (0.6 cm). The rock constituting the matrix is supposed inert with respect to  $\text{N}_2$ , i.e. without chemical reactivity.

The variations of relative permeability and capillary pressure according to water saturation are given in Figure 5. Relative permeability for aqueous ( $k_{rl}$ ) and gaseous ( $k_{rg}$ ) phases and capillary pressure ( $P_{cap}$ ) models are described according to the Van Genuchten formulation.

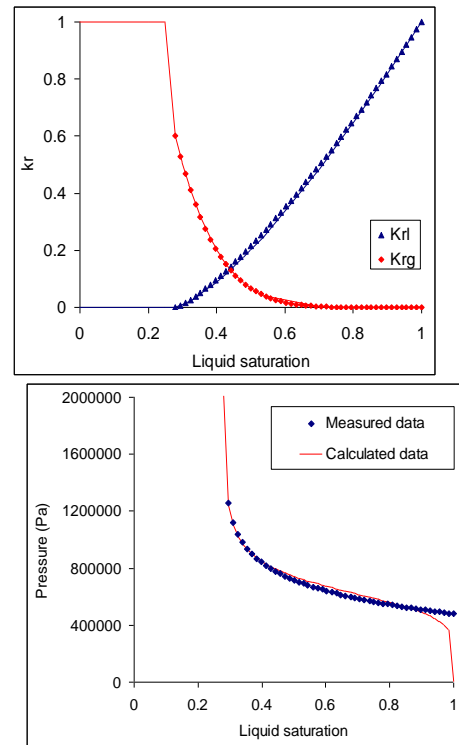


Figure 5. Relative permeability and capillary pressure curve according to water saturation ( $S_l$ ).

Due to the low permeability of the medium, we observe a very high sensitivity of the model to relative permeability and capillary pressure characteristics, in particular to the entry pressure. As shown by Figure 5, the Van Genuchten model does not fit properly the measured data when liquid saturation is close to 1. This very weak shift has an impact on the breakthrough time.

For "Grès de Môlière" rock, high pressure mercury injection and standard centrifugation have been done to measure the capillary pressure curve. The model parameters are deduced:  $S_{lr} = 0.22$ ,  $S_{gr} = 0.05$ ,  $P_0 = 645161$  Pa and  $m = 0.95$ .

When these parameters are correctly defined, the code can reproduce, with a good agreement, the first 3 stages of the experiment including the mean water saturation and the outlet gas flow rate (Figure 5).

These three first stages correspond to the desaturation of the porous medium according to a classical piston effect. The desaturation state is proportional to the pressure gradient applied to the core whereas the evaporation process is negligible: at the end of stage 3, the water content is close to the residual liquid saturation.

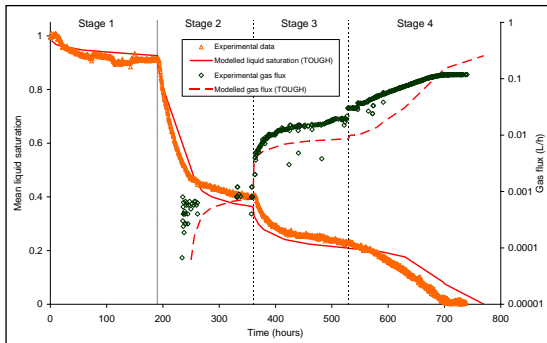


Figure 6. - Results of drying-out experiments with gaseous  $N_2$  at laboratory scale (Peysson et al. 2010) compared with results of numerical modeling performed with TOUGH2 code (André et al. 2010).

During the first 3 stages, the calculated average water saturation in the core fit quite well the measured data. Some discrepancies are observed close to the inlet and the outlet of the column which are mainly due to the selected boundary conditions imposed to the numerical model.

In the last stage (stage 4) desiccation of the medium is the dominant mechanisms. Even if

the global tendency is roughly reproduced, this stage presented some difficulties to reproduce correctly measured data.

Indeed, the only way to fit both gas flow rate and desiccation time consists to increase the gas permeability when liquid saturation is lower than the residual liquid saturation. By increasing the relative gas permeability, the outlet gas flow rate is growing; the evaporation process goes faster and the time needed to totally desiccate the core decreases. These numerical simulations of laboratory experiments at  $90^\circ C$  allow checking the relevance of the model but also the determination of the most sensitive and ad hoc parameters of the integrated approaches (optimized relative permeability and capillary pressure curves). Finally, the good coherence between measured and calculated data is very encouraging. We also demonstrated that the petrophysical parameters established at  $90^\circ C$  are applicable at  $120^\circ C$  without any adjustment for the same rock (André et al., 2010).

### Extrapolation at field scale (2D-radial approach)

When extrapolated to the near wellbore field and because of the gravity forces and the supercritical  $CO_2$  density (lower than the one of the brine), the reservoir desaturates faster at the top. The porous medium is dried on about 12 m at the reservoir top, whereas at the bottom, only the first meter is totally desiccated (Figure 7). Inside the drying zone, solid salt (i.e., halite) precipitates. If salt is present in all the desaturated zone, the spatial repartition of salt deposits varies according to the resultant prevalent transport forces (advection, diffusion, capillarity, evaporation, etc.) inside the reservoir: the amounts are higher at the bottom of the reservoir and more limited at the top for simulation conditions and specific characteristics of the reservoir. The pattern of solid saturation (= solid volume/pore volume) indicates that 40% of the porosity is occupied by salt at the bottom, whereas only 10% at the top is filled. The porosity and consequently the permeability are more impacted at the bottom of the reservoir (Figure 7). The permeability decrease is represented by the empirical function  $k_{red} (= k/k_0)$ . This function clearly shows that high permeability reductions are expected close to the well (skin effect in the first cell party with

the well) and at the lower part of the reservoir (in the first meter inside the reservoir).

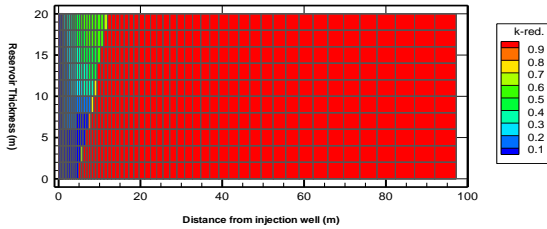


Figure 7. Permeability reduction,  $k_{red}$  ( $=k/k_0$ ) inside a 100 m radius around the injector well after ten years of  $CO_2$  injection.

At the end, we investigated specifically the influence of shutdown periods during the injection phase. Numerical simulations were performed considering the case of  $CO_2$  injection into an aquifer open with a nominal flow of  $1Mm^3/y$  and several short shutdown periods. Pc-Kr models were built to be fully representative of rock types with permeabilities of 10 and 100 mD for an integrated approach to ensure consistency between original K, Kr and Pc. The results show little effect related to re-imbibition layers well. The temporary shutdown of the wells does not seem to pose a major problem on the injectivity with a homogeneous model including hysteresis effects.

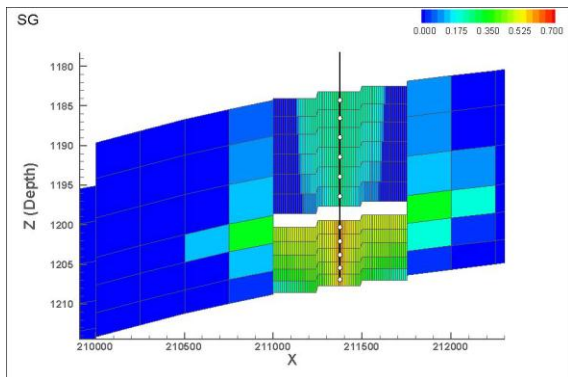


Figure 8. Vertical section illustrating the saturation tank of gas around the injection well for a mid-horizontal permeability 100mD (RT1) in the deep layers and 10mD (RT2) in the upper layers. This saturation state is the last day of the injection history, after six years of injections interrupted by two years of rest.

## CONCLUSIONS

For the flows in the wells, the numerical simulation results show trends highlighting the problem of "Injectivity gap" allowing a failure to achieve a controllable pressure range at the bottom of the injection well because of phase change in the injection well. The involvement of industrials (ie, Schlumberger, GDF Suez and Total) in the project brings validated injection scenarios thanks to the implementation of numerical tools.

Most of the efforts to study the mechanisms at the interfaces of geochemical phases ( $CO_2$ -brines) were focused on  $CO_2$  solubility in capillary water. Detailed speciation of carbonic acid is well established for the range of relative humidity and drying conditions studied in the project. A comprehensive approach for estimating the interfacial tension of the brine- $CO_2$  system, based on the theory of electrolytic systems was developed (Leroy et al., 2010).

Drying processes are investigated through laboratory experiments and numerical simulations to evaluate the dynamic of the water saturation decrease in sandstones and the consequences of induced salt depositions on the injectivity. We demonstrate that in low permeability porous media, the relative permeability of gas phase significantly increases when water saturation is lower than the irreducible water saturation. When this parameter is adjusted, the numerical code is able to reproduce the drying time and the outlet gas flow rate measured at laboratory scale on cores, using a two-phase Darcy flow and thermodynamic equilibrium between phases.

At field scale, the rocks characteristics defined at laboratory scale are used to predict the behaviour of the near-well zone according to the injection gas flow rate. We demonstrated that the precipitation process and the amount of salt deposits are related to different parameters:

- the salinity of the initial brine: the more concentrated the brine is, the more massive the salt deposit is;
- the irreducible water content: water entrapped in pores is evaporated by gas injection. The higher this content is, the more important the amount of precipitated salt is;



- the gas injection flow rate and the capillary forces within the system.

Finally, all these parameters have to be known (and defined) in order to improve the management of the long-term injection of CO<sub>2</sub> in the saline aquifers. According to the carried out reservoir simulations, several important results can be noted: i) for high permeabilities (> 100 mD), the mechanism of re-wetting of the aquifer is larger but no impact is observed in terms of injectivity because of high permeability; ii) for low-permeability media (<100 mD), the mechanism of re-imbibition is less marked and well find its ability to moderate injection after restart iii) the heterogeneities do not appear to play a major role in these findings and; iv) the key parameter is the curve of relative permeability to water. It is therefore recommended to measure this parameter accurately during the design phase.

#### **ACKNOWLEDGMENT**

This work is carried out within the framework of the “*Proche Puits*” project, co-funded by the French National Agency for Research (ANR). The authors are grateful to all project partners (TOTAL, GDF Suez, Schlumberger, Itasca, CNRS, University of Lorraine, and University of Pau) to allow the publication of this work.

#### **REFERENCES**

André L., P. Audigane, M. Azaroual, and A. Menjoz, Numerical modeling of fluid-rock chemical interactions at the supercritical CO<sub>2</sub>-liquid interface during supercritical carbon dioxide injection into a carbonated reservoir, the Dogger aquifer (Paris Basin, France). *Energ. Conv. Manage.*, 48, 1782-1797, 2007.

André, L., M. Azaroual, and A. Menjoz, Numerical Simulations of the Thermal Impact of Supercritical CO<sub>2</sub> Injection on Chemical Reactivity in a Carbonate Saline Reservoir. *Transp. Porous Med.*, 82, 247-274, 2010.

Gaus I., M. Azaroual, and I. Czernichowski-Lauriol, Reactive transport modelling of the impact of CO<sub>2</sub> injection on the clayey caprock at Sleipner (North Sea). *Chem. Geol.*, 217, 319-337, 2005.

Incropera F.P., De Witt D.P., (2001) Fundamentals of heat & mass transfer (5th

edition), John Wiley and Sons, 980p.

Leroy, P., Lassin, A., Azaroual, M., and André, L., (2010). Predicting the surface tension of aqueous 1:1 electrolyte solutions at high salinity. *Geochimica et Cosmochimica Acta* 74, 5427-5442.

Oldenburg C.M., Moridis G.J., Spycher N., Pruess K., 2004. EOS7C Version 1.0: TOUGH2 Module for Carbon Dioxide or Nitrogen in Natural Gas (Methane) Reservoirs. *Lawrence Berkeley National Laboratory Report LBNL-56589*, Berkeley, CA (USA).

Pruess K., C.M. Oldenburg, and G.J. Moridis, TOUGH2 User's Guide, Version 2.0. *Lawrence Berkeley National Laboratory Report LBNL-43134*, Berkeley, CA (USA), 1999.

Verma A., and K. Pruess, Thermohydrologic conditions and silica redistribution near high-level nuclear wastes emplaced in saturated geological formations, *J. Geophys. Res.*, 93(B2), 1159–1173, 1988.

Xu T., and K. Pruess, Modeling multiphase non-isothermal fluid flow and reactive geochemical transport in variably saturated fractured rocks: 1. Methodology, *Am. J. Sci.*, 301, 16-33, 2001.

Peysson Y., Bazin B., Magnier C., Kohler E., Youssef S., 2010. Permeability alteration due to salt precipitation driven by drying in the context of CO<sub>2</sub> injection. International Conference on Greenhouse Gas Technologies (GHGT-10), Amsterdam, 19-23 September 2010.

Mahadevan J., 2005. Flow-through drying of porous media. *PhD Dissertation*. The University of Texas at Austin.

Mahadevan J., Sharma M.M., Yortsos Y.C., 2007. Water removal from porous media by gas injection: experiments and simulation. *Transport in Porous Media*, 66, p. 287-309.

Kleinitz W., Dietzsch G., Köhler M., 2003. Halite scale formation in gas producing wells. *Chemical Engineering Research and Design* 81 (PartA).

Zeidouni M., Pooladi-Darvish M., Keith D., 2009. Analytical solution to evaluate salt precipitation during CO<sub>2</sub> injection in saline aquifers, *International Journal of Greenhouse Gas Control*, 3, p. 600–611